Titration-Based Screening for Evaluation of Natural Product Extracts: Identification of an Aspulvinone Family of Luciferase Inhibitors

Patricia G. Cruz,[1,9] Douglas S. Auld,[5,10] Pamela J. Schultz,[1] Scott Lovell,[6] Kevin P. Battaile,[7] Ryan MacArthur,[5] Min Shen,[5] Giselle Tamayo-Castillo,[8] James Inglese,[5,*] and David H. Sherman[1,2,3,4,*]

[1]Life Sciences Institute
[2]Department of Medicinal Chemistry
[3]Department of Chemistry
[4]Department of Microbiology & Immunology
University of Michigan, Ann Arbor, MI 48109-2216, USA
[5]NIH Chemical Genomics Center, National Human Genome Research Institute, NIH, Bethesda, MD 20892-3370, USA
[6]Protein Structure Laboratory, University of Kansas, Del Shankel Structural Biology Center, Lawrence, KS 66047, USA
[7]IMCA-CAT, Hauptman-Woodward Medical Research Institute, Argonne National Laboratory 9700 S. Cass Avenue, Building 435A, Argonne, IL 60439, USA
[8]Unidad Estrategica de Bioprospeccion, Instituto Nacional de Biodiversidad (INBio), Santo Domingo de Heredia, Costa Rica & Escuela de Química, Universidad de Costa Rica, 2060 San Pedro, Costa Rica
[9]Present address: Pharma Mar, Avda. de los Reyes, 1 P.I. La Mina-Norte, Colmenar Viejo, Madrid 28770, Spain
[10]Present address: Novartis Institutes for BioMedical Research Center for Proteomic Chemistry, 250 Massachusetts Avenue, Cambridge, MA 02139, USA
*Correspondence: jinglese@mail.nih.gov (J.I.), davidhs@umich.edu (D.H.S.)
DOI 10.1016/j.chembiol.2011.08.011

SUMMARY

The chemical diversity of nature has tremendous potential for the discovery of molecular probes and medicinal agents. However, sensitivity of HTS assays to interfering components of crude extracts derived from plants, and macro- and microorganisms has curtailed their use in lead discovery. Here, we describe a process for leveraging the concentration-response curves obtained from quantitative HTS to improve the initial selection of "actives" from a library of partially fractionated natural product extracts derived from marine actinomycetes and fungi. By using pharmacological activity, the first-pass CRC paradigm improves the probability that labor-intensive subsequent steps of reculturing, extraction, and bioassay-guided isolation of active component(s) target the most promising strains and growth conditions. We illustrate how this process identified a family of fungal metabolites as potent inhibitors of firefly luciferase, subsequently resolved in molecular detail by X-ray crystallography.

INTRODUCTION

Natural products (NPs) are unparalleled in representation among both drugs and chemical probes, and as many as 63% of the new chemical entities for drugs discovered between 1981 and 2006 have been traced to or based on these structurally diverse secondary metabolites (Carlson, 2010; Newman, 2008; Newman and Cragg, 2009). Recent studies have revealed that 34 NP-based drugs have been approved between 1998 and 2007 (Butler, 2008). However, naturally-derived small molecules have received less attention in recent years, due in part to the laborious process involved in identification, isolation, and follow-up compared to leads derived from synthetic libraries (Li and Vederas, 2009). Screening of NP libraries often included a time-demanding workflow of deconvolution, and validation that became unsustainable when compared to the timelines achievable from HTS of synthetic chemical libraries. Paradoxically, despite the prevalence of NPs among successful drugs and powerful chemical probes, this burden resulted in the curtailing or termination of NP extract (NPE)-based discovery efforts at many pharmaceutical companies over the last decade (Harvey, 2007; Koehn and Carter, 2005; Lam, 2007; Newman, 2008).

To sample maximum chemical diversity in NPE-based screening, the library should remain sufficiently rich in chemical matter but devoid of undesirable characteristics that make it difficult to test with highly sensitive HTS assays (Harvey, 2007; Inglese et al., 2007; Koehn and Carter, 2005). For this reason we focused on NPE libraries where partial or prefractionation of the crude extracts was accomplished and accompanied by elution profile data. Fractionated extracts help reduce or eliminate artifacts associated with crude material. For example, crude organic solvent extracts are relatively straightforward to prepare, but the high concentrations of salts, pigments, and polymeric constituents can interfere significantly with sensitive detection outputs of modern HTS. Compound-mediated phenomena complicating the interpretation of HTS data are becoming increasingly well characterized (Baell and Holloway, 2010; Inglese et al., 2007; Thorne et al., 2010a).

To improve efficiency of NP identification, we explored a new strategy that integrates recent advances in HTS and NPE library
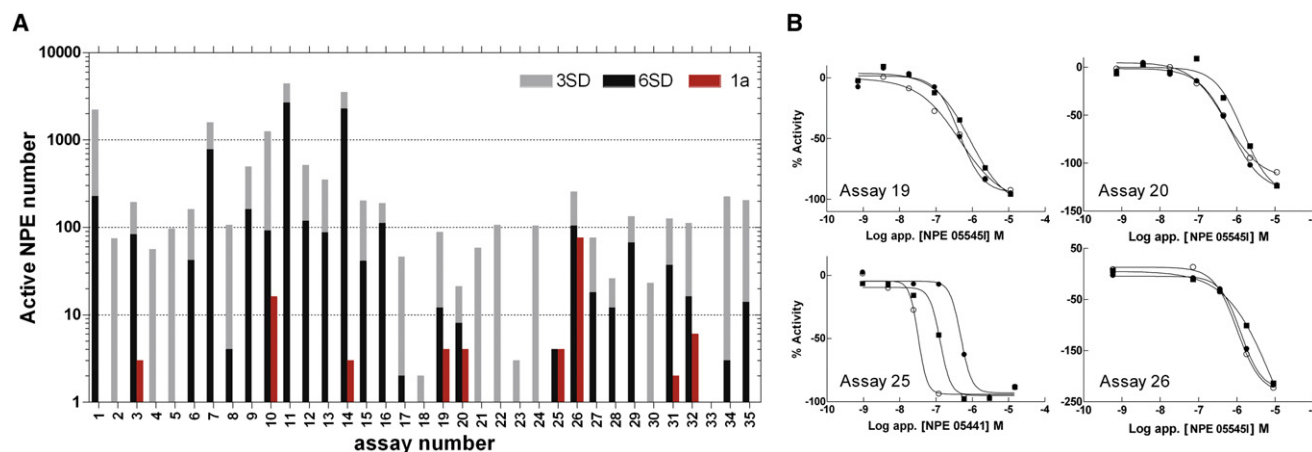
Figure 1. Activity Analysis of NPEs in Various Assays

(A) Bar chart summarizing active NPEs in assays ordered by format: 1–15 are fluorogenic; 16–18 are fluorescent polarization; 19–30 are bioluminescent; 31–32 ALPHA-based chemiluminescent; 33–34 use fluorescent protein expression; and 35 is an absorbance output. The number of active NPEs per assay is indicated on the y axis, where red represents a class 1a CRC (as previously defined [Inglese et al., 2006]), whereas 3 SD and 6 SD cutoffs for activity at a single apparent concentration of 10 μM are given by the gray and black bars. One class 1a CRC falls in assay 29, see Table S1.

(B) Plots showing qHTS class 1a CRC results from assays selected for further analysis (see also Figure S2B). Assays 19, 20, and 26 displayed activity from a common strain, NPE 05545.

Additional assay details can be found in Table S1.

production to enable a more efficient means of isolating active components from NP sources. Specifically, we chose "prefractionated" NPEs from culturable microorganisms that are prepared by differential solvent extraction of initially XAD resin-bound NPEs into three "prefractions" that are transferred to a 384-well plate (see Figure S1A available online). We also employed a titration-based screening paradigm, quantitative HTS (qHTS) (Inglese et al., 2006), where samples in large chemical libraries can be rapidly tested at different concentrations, and concentration-response curves (CRCs) are fitted to the data. Titration of the different solvent extractions provides a further dimension of resolution where pharmacological activity of the CRCs is correlated with the NPE elution profile data. Furthermore, in such an approach samples can be formatted into a 1536-well-based titration archive suitable for rapid screening (Figure S1B) (Yasgar et al., 2008). The use of a CRC classification scheme (Inglese et al., 2006; Shukla et al., 2009), derived from qHTS to select active wells, provides a unique means to track active components in association with the sample elution profile, and provides higher confidence data to ensure that typical HTS artifacts are largely avoided. A successful major effort using our screening paradigm could reinitiate and improve the application of this fertile area of NP chemical probe and drug discovery. Here, we report our methodology and initial validation involving qHTS in the testing of NPE libraries derived from Costa Rica marine microbial resources.

RESULTS

Evaluation of an NPE Library by qHTS

In an effort to improve the process of identifying biological activity from NPE libraries, we tested extracts in qHTS format across 35 diverse assays that were optimized for 1536-well format (Table S1). To reduce the ionic, optical, and aggrega-

tion-based interference from high-salt concentration, pigments, polymeric organics, and other resinous materials, we prepared the extracts using XAD resin to enrich the NPs from these genetically diverse and pure culture actinomycete and fungal strains while reducing the content of biomass at the extremes of polarity (e.g., nonorganic or highly lipophilic).

The NPE library we subsequently prepared for qHTS contained 15,704 samples that comprised 13 separate 7-concentration inter-plate titration series, such that overall, 91 individual 1536-well plates were maintained as a titration archive for screening (Figure S1B). As a dynamic library that increases in size over time, a subset of the archived library (~5300 samples) was tested in the diverse assay panel to estimate the relative activity of the extracts. By examining data from a single-tested concentration, qHTS data can also be examined as a traditional single-point high-throughput screen. A retrospective analysis of the activity from the preliminary testing of the NPE library across the assays in this manner resulted in a broad range of activity from none to several thousand actives (Figure 1A) at either 3 or 6 standard deviations (SDs) as a cutoff for biological activity. From this subset, "hit" rates spanning 0%–80% for 3SD or an average of 11%, and 0%–50% for 6 SD or average of 4.5% were observed. The highest hit rates, those above 5% (3 SD), were all limited to biochemical assays except for one that measured cellular viability (assay 26, Figure 1A). Using qHTS analysis among the assays tested, 10 gave high-quality class 1a CRCs (Figures 1A and 1B). These assays were comprised of 2 cell-based assays and 8 biochemical assays that employed detection formats of fluorescence, absorbance, and bioluminescence, with 5 of the 10 based on firefly luciferase (FLuc) outputs. Initially, we decided to follow up actives from screens employing purified molecular targets, based primarily on a high-quality pharmacological response in a single assay. A particular extract (Papua New Guinea 05441) with high apparent potency 1a
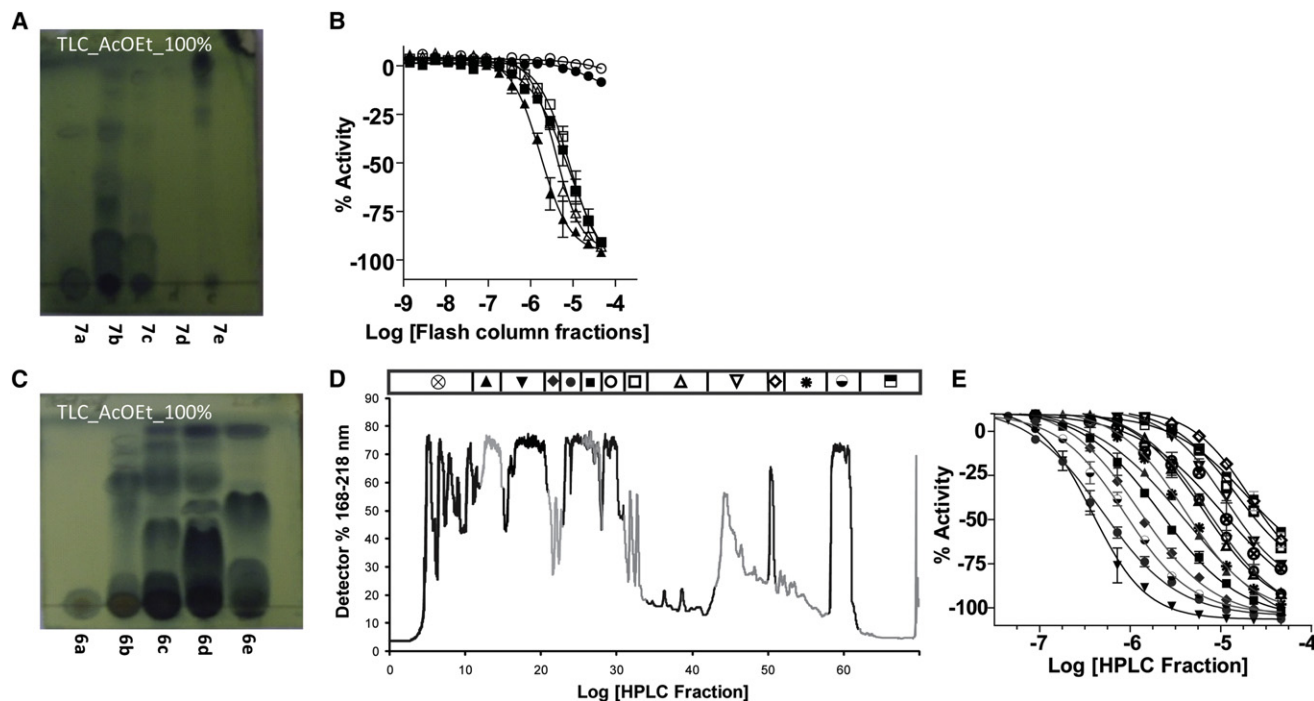
Figure 2. Bioactivity-Guided Dereplication of NPE 05545

(A) Thin-layer chromatography analysis of flash-column fractions from an acetone extract of XAD-16-bound culture extract from strain 05545.

(B) Activity of flash-column fractions shown in (A) in FLuc enzyme assay (open square, X+A; solid triangle, 7a; open triangle, 7b, closed square, 7c; solid circle, 7d; open circle, 7e).

(C) Thin-layer chromatography analysis of flash-column fractions from an independent culture of 05545.

(D) Reverse HPLC of the components of flash column fraction 6c in (C).

(E) Activity from the HPLC separation shown in (C).

curves in all three solvent extracts was identified for Calmodulin Kinase IIa (assay #25; Figures 1A and 1B); however, a retest with a new extract from the same strain did not yield the original activity (Figure S2A), illustrating the challenges of working with uncharacterized mixtures and the importance of initial selection criteria limiting the number of follow-ups. However, several assays (#19, #20, #26) based on a common FLuc output showed CRCs from a number of NPEs, suggesting to us that these NPEs potentially contained FLuc inhibitors (Figure 1; Figure S2B). However, more restricted in prevalence were class 1a CRCs (e.g., Costa Rica strain 05545 and 06085). Using this observation to strengthen the commitment to proceed with dereplication, we recultured strain 05545 and initiated the isolation of the active constituents of this NPE (Figure 2).

Structural Characterization of a Series of Aspulvinones

The strain 05545, a marine fungus from the genus *Aspergillus* (determined by 18S rRNA gene sequence analysis; data not shown), was isolated from Costa Rica marine sediments, collected in Isla Despensa, Guanacaste Conservation Area in December 2005. The terrestrial *Aspergillus* sp. is known by the production of pulvinone derivatives, unsaturated tetronic acids with an aryl substituent at C2, an arylmethylene substituent at C4, and isoprene residues in the aryl rings (Ojima et al., 1975).

The marine fungus was scaled-up to 5 l, and the active extracts were subjected to chromatographic separation using

a combination of MPLC and HPLC (Figure 2). The fractionation of active extracts was followed by secondary bioassay to guide isolation of six new derivatives, aspulvinones I-CR to M-CR (**4–9**), in addition to known aspulvinones E, F, and H (**1–3**) (Sugiyama et al., 1979; Ojima et al., 1975), as well as butyrolactone I and III (**10** and **11**) (Rao et al., 2000; Parvatkar et al., 2009; Niu et al., 2008) and benzofuran (**12**) (Donnelly et al., 1988; Huang et al., 2008) (Figure 3). Aspulvinone F (**2**) was reported in 1975 with an incorrect structure (Ojima et al., 1975), and in 1979 it was reconsidered by Begley et al. (1979), who suggested that aspulvinone F likely bears a dihydrofuran ring instead of an epoxide. Our NMR data and X-ray crystallographic analysis reveal that the proposed revised structure is formally confirmed, and the absolute configuration of the chiral center was established as R (Figures 4A and 4B).

Aspulvinone I-CR (**4**) was isolated as a pale-yellow solid. The HREIMS gave an $[M]^-$ ion at m/z 479.1659, consistent with the molecular formula $C_{27}H_{28}O_8$, requiring 14 sites of unsaturation and 16 amu more than compound **2** ($C_{27}H_{28}O_7$). The ^{1}H-NMR and ^{13}C-NMR data indicated that the structure of **4** is very similar to compound **2**. The most significant differences in the NMR data reside in the high-field shift effect of the signal at C-23 (δ_H 3.19, δ_C 31.8) and the presence of a sp^3 methine instead of a sp^3 methylene at C-24, (δ_H 4.61, δ_C 91.4). These data indicated that compound **4** bears a dihydrofuran ring fused to the benzene ring, as opposed to the dihydropyran ring present
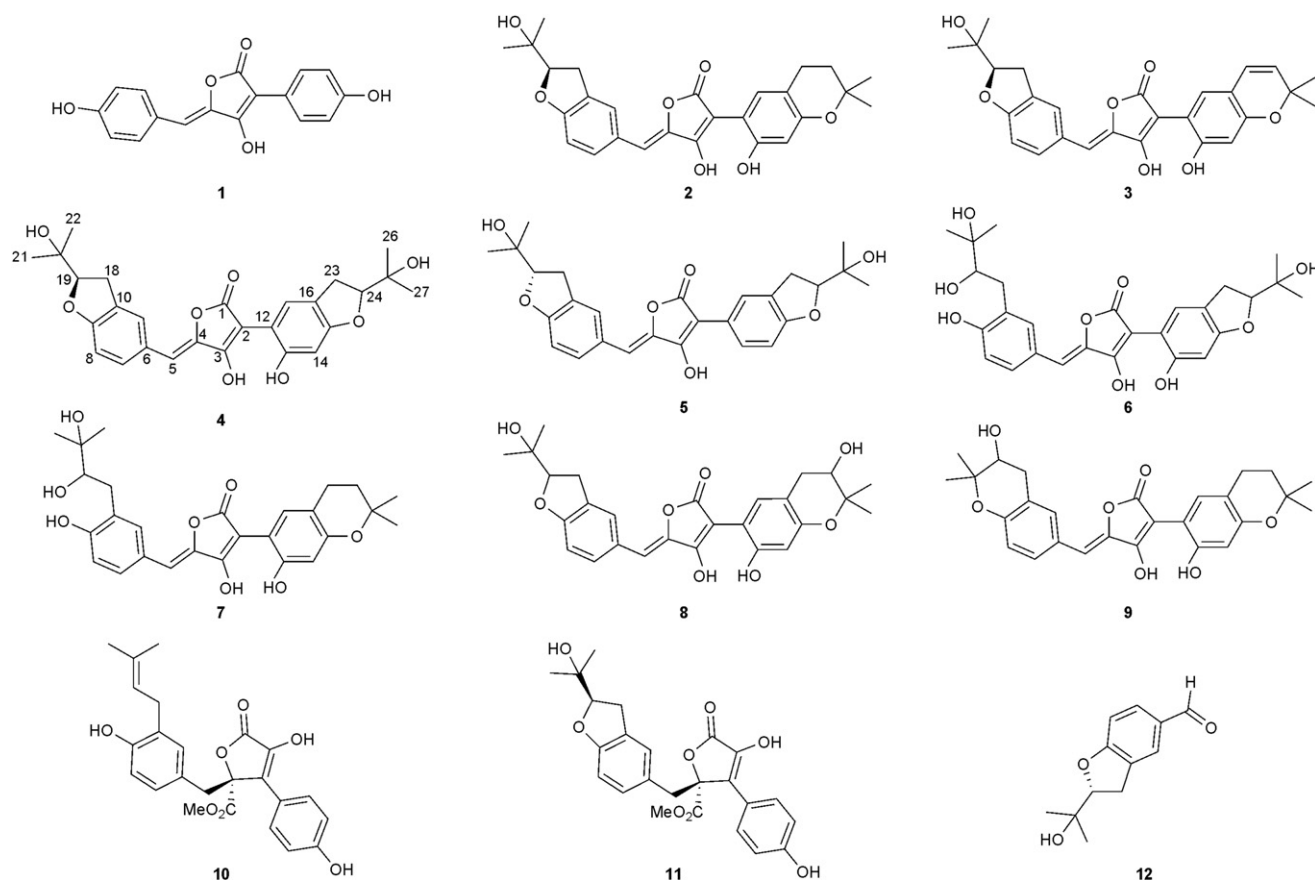
Figure 3. Structures of Isolated Metabolites

Aspulvinone E (**1**), aspulvinone F (**2**), aspulvinone H (**3**), aspulvinone I-CR (**4**), aspulvinone J-CR (**5**), aspulvinone K-CR (**6**), aspulvinone L-CR (**7**), aspulvinone M-CR (**8**), aspulvinone N-CR (**9**), butyrolactone I (**10**), butyrolactone III (**11**), and benzofuran (**12**). ^{1}H- and ^{13}C-NMR, COSY, and HSQC spectra for compounds **2** and **4–9** are provided in Figures S4–S31 and Tables S3 and S4.

in compound **2**. This structure was further supported by COSY, HSQC, and HMBC spectra. COSY correlations between H_2-23 and H-24, as well as between H_2-18 and H-19, supported the presence of two dihydrofuran ring systems. HMBC correlation from H_2-18 to C-9 and C-10, H-8 to C-10, H-7, and H-11 to C-9, H_2-23 to C-15 and C-17, and H-17 to C-23 confirmed the presence of a dihydrofuran fused to each of the benzene rings.

Aspulvinone J-CR (**5**) was obtained as a pale-yellow solid. Its molecular formula $C_{27}H_{28}O_7$ was established by HREIMS [M+Na]$^+$ ion at 487.1733, indicating 14 degrees of unsaturation. The NMR features of **5** were similar to those of **4** except that the right-hand benzene ring is trisubstituted, showing a sp^2 methine at C-13 in **5** (δ_H 7.81, δ_C 127.8). A COSY cross-peak between H-13 and H-14 as well as HMBC correlations between H-13 and C-2, C-11 and C-15 confirmed these assignments. These assignments were reconfirmed by cocrystal structure of **5** with the FLuc (see below).

Aspulvinone K-CR (**6**) was isolated as a brown-yellow optically active oil. The [M+Na]$^+$ ion at m/z 521.1788 in the HREIMS suggested $C_{27}H_{30}O_9$ as the molecular formula, which indicated 18 additional amu, with 1 less unsaturation site than compound **4**. A significant change in the ^{1}H-NMR and ^{13}C-NMR was also observed in the methine C-19, which shifted from δ_H 4.63 and

δ_C 90.7 in **4** to δ_H 3.64 and δ_C 79.8 in **6**. These modifications together with the shift of C-9, from δ_C 161.0 in **4** to δ_C 157.2 in **6**, suggested that there are a hydroxyl and 2,3-dihydroxy-3-methylbutyl group upon C-9 and C-10, respectively, instead of the dihydrofuran ring.

Aspulvinone L-CR (**7**) isolated as a yellow oil gave a [M+Na]$^+$ ion at m/z 505.1838 in the positive ion HREIMS, consistent with the molecular formula of $C_{27}H_{30}O_8$, and requiring one less unsaturation site than compound **2**. NMR data of compound **7** were similar to those of compound **2** except for C-18 and C-19. The shifts of C-18 from δ_H 3.18 and δ_C 30.0 in **2** to δ_H 2.96, 2.66 and δ_C 34.8 in **7**, as well as the change in C-19 from δ_H 4.60 and δ_C 89.9 in **2** to δ_H 3.63 and δ_C 81.1 in **7**, suggests that in this compound the formation of the dihydrofuran ring did not occur. Instead, there is the open form where C-10 bears a 2,3-dihydroxy-3-methylbutyl group, as in compound **6**.

Aspulvinone M-CR (**8**) was isolated as a yellow solid. The HREIMS gave an [M+Na]$^+$ ion at m/z 503.1682, consistent with the molecular formula $C_{27}H_{28}O_8$ and the same degrees of unsaturation as compound **2**. The only difference compared with compound **2** was the shift of C-24 from δ_H 1.77 and δ_C 33.3 in **2** to δ_H 3.72 and δ_C 71.0 in **8** due to a secondary hydroxyl group at C-24.
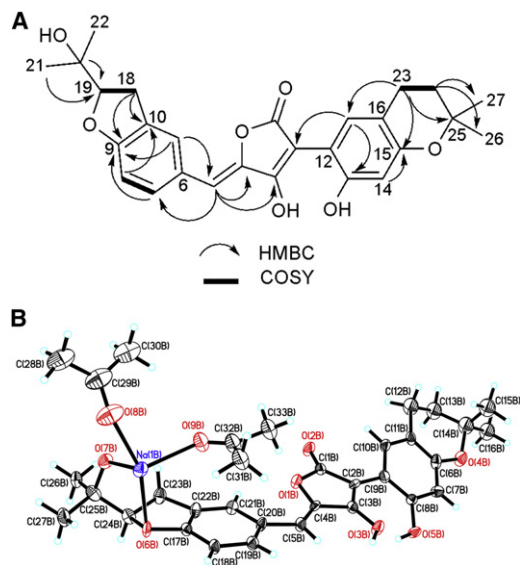
A

B

Figure 4. NMR and X-ray Analysis of Aspulvinone F (2)
(A) Key ^{1}H-^{1}H COSY and HMBC correlations observed in **2**.
(B) X-ray structure of **2**. Perspective views showing 50% probability displacement ellipsoids of an independent aspulvinone F molecule. Na$^+$ is chelated with four oxygens, two from acetone molecules, and two from aspulvinone F (**2**). Carbon atoms are shown in black, oxygen atoms in red, protons in white, and Na$^+$ in blue.

Table 1. Aspulvinone Analogs Tested against Five Luciferase Variants

Cmp	FLuc	LmLuc	Ultra	RLuc	VLuc
1	1.4 ± 1.6	3.6 ± 1.1	0.76 ± 0.12	Inactive	>57
2	3.6 ± 1.5	2.5 ± 0.5	>57	>57	Inactive
3	1.8 ± 0.9	1.9 ± 0.8	19.0 ± 4.6	>57	>57
4	0.72 ± 0.40	0.50 ± 0.20	4.1 ± 1.8	Inactive	12.0 ± 2.3
5	0.1 ± 0.02	0.1 ± 0.03	4.5 ± 3.8	>57	6.5 ± 3.3
8	1.7 ± 1.6	5.3 ± 5.9	33 ± 2.1	Inactive	18 ± 8
10	Inactive	Inactive	Inactive	>57	>57
11	Inactive	Inactive	Inactive	Inactive	>57
12	18.6 ± 8.8	14.8 ± 2.8	31.7 ± 3.0	Inactive	Inactive

Data are mean ± SD values, from at least four determinations. All values are in micromolar (μM). >57, percent (%) inhibition between 20% and 50% at the highest tested concentration of 57 μM; Inactive, percent (%) inhibition <20% observed at the highest tested concentration. FLuc, *Photinus pyralis* luciferase. Related luciferases: LmLuc, *Luciola mingrelica* luciferase (82% identical); Ultra, Ultra-Glo luciferase (derived from *Photuris pennsylvanica* [68% identical]). Unrelated luciferases: RLuc, *Renilla reniformis* luciferase; VLuc, *Vibrio fischeri* luciferase (Ye et al., 1997).

in the five- or six-membered ring heterocycles. Whether this represents a common biosynthetic theme that includes pyran ring formation in the notoamide/stephacidin/paraherquamide class of fungal-derived alkaloid NPs remains to be explored in detail (Ding et al., 2010).

Specificity of Aspulvinone Activity

The aspulvinones demonstrated a wide range of activity across five luciferase species and variants (Table 1). Two of these luciferases (LmLuc and Ultra-Glo) were related to the commonly utilized luciferase derived from *Photinus pyralis* (FLuc), and two were unrelated luciferases that accommodate different substrates and enzymatic mechanisms to produce bioluminescence (RLuc and VLuc). Analogs of the NP displayed binding affinity for the related luciferases FLuc, LmLuc, and the thermostable (Ultra-Glo; Promega) FLucs in the submicromolar range, whereas potencies decreased to undetectable for the two species of luciferases that were genetically unrelated to FLuc.

X-ray Cocrystal of Aspulvinone J-CR Bound to FLuc

To further characterize the physical interaction of the aspulvinone series with FLuc, apo crystals of the *Photinus pyralis* luciferase protein were soaked in the presence of aspulvinone J-CR (**5**), one of the more potent aspulvinone congeners (Table 1). Following structural determination by molecular replacement and subsequent refinement to a resolution of 1.7 Å, the resulting electron density maps were examined for ligand binding. Aspulvinone J-CR (**5**) was clearly bound as prominent difference electron density (Fo-Fc), greater than 3σ was observed, which was consistent with this compound (Figure 5B).

Aspulvinone J-CR (**5**) fully occupies the D-luciferin binding site with the isopropyl alcohol at one terminus of the structure positioning deeply into the D-luciferin binding pocket and the other isopropyl alcohol extending into the ATP-binding site (Figure 5A). The aspulvinone molecule adopts a mostly planar
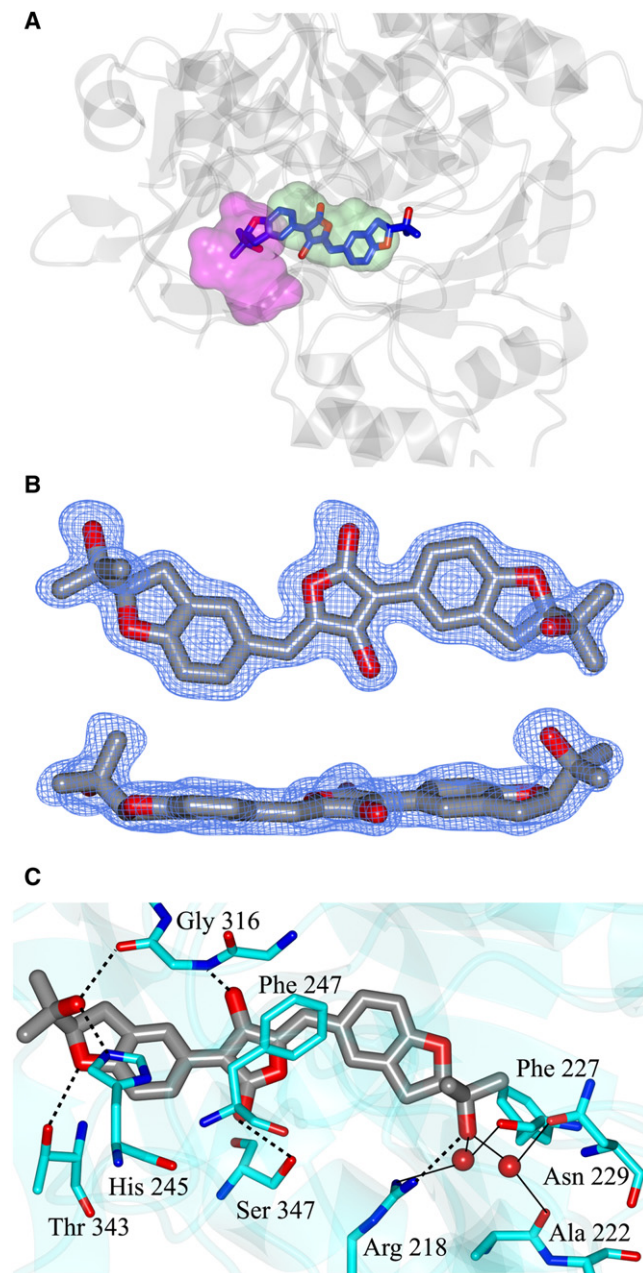
Aspulvinone N-CR (**9**) was obtained as a yellow crystalline oil with the molecular formula $C_{27}H_{28}O_7$ on the basis of HREIMS data, [M+H]$^+$ ion at m/z 465.1913. The level of unsaturation is the same as in compound **2**, but the difference in the shifts of methylene C-18 and methine C-19 indicated the presence of a dihydropyran with a hydroxyl group at C-19 instead of the dihydrofuran ring present in **2**. Compared with **2,** compound **9** showed shifts in the signal H$_2$-18 from δ$_H$ 3.18 to 3.03, 2.72, and H-19 signal shifted from δ$_H$ 4.60 to 3.75. Also, the ^{13}C signals of C-18 and C-19 shifted from δ$_C$ 89.9 to 68.7 and from δ$_C$ 71.1 to 77.2, respectively. COSY correlations between H$_2$-18 and H-19 and HMBC correlations between H$_2$-18 and C-9, C-10, C-11, C-19, and C-20, as well as between H-19 with C-10, C-18, C-21, and C-22 were consistent with a hydroxyl group at C-19.

Pulvinones **11–12** (Sugiyama et al., 1979; Rao et al., 2000; Ojima et al., 1975; Parvatkar et al., 2009) have been isolated from terrestrial and marine *Aspergillus* species, whereas **1–3** (Sugiyama et al., 1979; Niu et al., 2008) only from the terrestrial fungus. Here, we report the isolation of aspulvinones **1–9** from a marine *Aspergillus* sp., indicating that although derived from a completely different environment, this fungus maintains the capacity for synthesizing this class of compounds.

The aspulvinone family of NPs has a more complex carbon framework than the related pulvinones due to the incorporation of two isoprene units. The *ortho* position to the hydroxyl group serves as the site for alkylation by a dimethylallyl diphosphate mediated by a presumed prenyltransferase. Based on isolation of aspulvinones K-CR and L-CR (compounds **6** and **7**), we surmise that prenylation is followed by epoxidation or dihydroxylation of the double bond with subsequent cyclization, resulting

Figure 5. Structure of FLuc containing bound aspulvinone J-CR (5)

(A) View of **5** (blue and red cylinders) in the active site of luciferase (gray ribbons). The ATP and luciferin-binding regions are colored magenta and green, respectively.

(B) Two views of the Fo–Fc electron density map for **5** contoured at 3 sσ.

(C) Hydrogen bonding between **5** (gray/red) and luciferase (cyan). Water molecules are drawn as red spheres. Direct contacts between luciferase and **5** are shown as dashed lines, and water-mediated interactions are indicated by the solid lines. Crystallographic data for **5** can be found in Table S2.

arrangement across the three-ring system. However, the plane of the benzofuran ring that is positioned in the D-luciferin binding region is angled 18.9° relative to the mean plane defined by the hydroxyl-butyrolactone core (Figure 5B). The benzofuran ring in

the ATP-binding region is only 5.8° relative to the hydroxyl-butyrolactone mean plane. The isopropyl termini are oriented on the same side of the three-ring system. In general the driving force of aspulvinone binding to luciferase is highly enriched by hydrogen bond interactions (Figure 5C). Two oxygen atoms of the hydroxyl-butyrolactone core are able to form hydrogen bonds to the backbone—NH of Gly316 and the hydroxyl group of Ser347, with the optimal H-bonding distance of 2.73 and 2.85 Å, respectively. Notably, the isopropyl alcohol on both ends of the aspulvinone J-CR (**5**) structure could form tight binding with the surrounding residues through a hydrogen bond matrix. The one fitting deeply into the D-luciferin binding pocket forms a direct hydrogen bond to Arg218 and also a few water-mediated hydrogen bonds to Arg218, Ala222, Phe227, and Asn229 through two structural water molecules. In contrast the other isopropyl alcohol extending into the AMP-binding site is involved in hydrogen bonding with His245 and the backbone carbonyl oxygen of Gly316. Additionally, the oxygen of the dihydrobenzofuran ring could further help the molecule lock on the correct binding mode through the hydrogen bond interaction to Thr343.

Based on the cocrystal structure of FLuc with aspulvinone J-CR (**5**), we further examined aspulvinone F (**2**), which is ~30-fold less potent than **5** as a FLuc inhibitor (Table 1). The docking model of **2** indicated that it could adopt the same binding orientation and maintain nearly all key interactions as **5**. However, the isopropyl alcohol extending into the AMP-binding site was missing in **2**. Because this isopropyl alcohol forms hydrogen bonds with His245 and the backbone carbonyl oxygen of Gly316 in **5**, the absence of such a moiety in **2** could explain this significant potency shift (Figure S32).

In a previous study we elucidated inhibitor-based protein stabilization as the mechanism by which the small molecule PTC124 increases the activity of a FLuc reporter protein used in an assay designed to discover nonsense codon-suppressor compounds (Auld et al., 2008a, 2009a). We found that PTC124 stabilized the half-life of the enzyme by reacting at the FLuc active site with ATP to form a multi-substrate adduct inhibitor (MAI), which we determined from crystallographic studies (Auld et al., 2010; Thorne et al., 2010b). This potent inhibitor can be displaced from the enzyme through the use of typical luciferase detection reagents that contain high concentrations of substrates including CoASH, which presumably thiolytically cleaves the MAI (Auld et al., 2010), thus allowing detection of FLuc enzyme activity in the assay. The PTC124-AMP adduct effectively fills the active site of FLuc. Alignment of the aspulvinone cocrystal structure and the structure of PTC124-AMP adduct in the luciferase active site revealed a similar binding orientation in the D-luciferin pocket (Figure 6). The hydroxyl-butyrolactone core of aspulvinone occupies a similar position to the oxadiazole of PTC124. However, it was found that the central ring system of aspulvinone J-CR forms an angle of 50.8° between the mean planes defined by the butyrolactone ring (five membered) and the aryl ring of Phe247. This is too large for a π-π (face-to-face, quadrupole-quadrupole) interaction or the aromatic stacking observed in the PTC124-AMP-FLuc structure, and more closely approximates a herringbone (edge-to-face, dipole-quadrupole) interaction (Burley and Petsko, 1985, 1988). The planar nature of both ligands makes the molecules
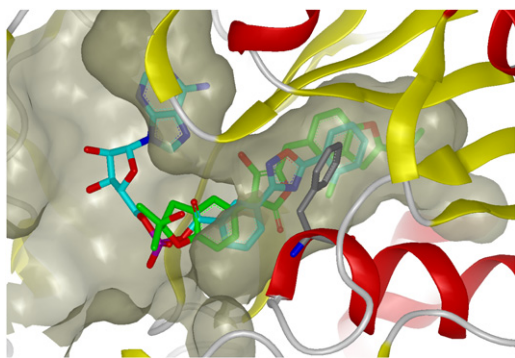
Figure 6. Superposition of Aspulvinone J-CR (5) and PTC124-AMP Adduct within FLuc-Binding Pocket

Protein is shown in ribbon representation, and the binding pocket is depicted by molecular surface, **5** is shown in green, and PTC124-AMP is shown in cyan. Phe247 is shown in gray. This figure was prepared with the program VIDA (OpenEye Scientific Software).

well accommodated in the unusually long and linear binding pocket of D-luciferin.

DISCUSSION

Selection of initial NPEs for bioassay-guided fractionation was considered carefully given the considerable effort in dereplication required for each follow-up. Our primary consideration was an apparent pharmacological response, as indicated by high-quality CRCs from one or more of the three solvent extracts. Data of this character were significantly more discriminating than activity based on a threshold inhibition (e.g., compare analysis of percent [%] activity versus high-quality curve class activity in Figure 1A), where even a low false-positive rate can lead to unacceptable confirmation rates. In addition, given the rare and unique nature of the NPE samples, we employed the qHTS approach to measure the activity in as comprehensive a manner as possible. Comparison of assays using a common detection technology allowed us to flag extracts that interfered with the detection output and also enabled the identification of the specific FLuc inhibitors shown in this study. However, in general the diversity of detection modalities, assay formats, and conditions employed across the sample of MLPCN assays surveyed here limited our ability to make optimal use of qHTS data to ascertain whether a CRC was the result of a pharmacologically mediated event or resulted from compound-mediated interference in the assay format or detection modality (Inglese et al., 2006; Thorne et al., 2010b).

Based on these findings, it is evident that another criterion for follow-up should be whether an NPE is either independently observed in several cross-validating or orthogonal assay formats having a common target, or is differentially active within a series of targets tested in a common assay platform. Coupled with a qHTS approach, assay panels that provide such a reinforcing or contrasting result should further improve the efficiency and probability of identifying isolable-active compounds. In the present study this approach led us to three assays in which high-quality CRCs were observed where the common target was FLuc. Dereplication of the active extract proceeded in a straightforward manner, leading to the isolation of several

new aspulvinone congeners. Follow-up studies against a series of bioluminescent enzymes demonstrated that these molecules are specific for bioluminescent enzymes related to the wild-type variety of FLucs. The lower overall activity against Ultra-Glo luciferase is consistent with a previous study that suggested a more restricted inhibitor profile with this thermostable optimized luciferase (Auld et al., 2009b).

The molecular basis for the high potency and selectivity of aspulvinone J-CR (**5**) toward FLuc is revealed in the X-ray cocrystal structure. Here, a flat planar structure that binds largely to the D-luciferin pocket but also can span into the AMP pocket is observed. The general structural architecture of the aspulvinone core bears some resemblance to the diaryl oxidazole found in molecules like PTC124, which bind to the luciferin pocket of FLuc, both using a heteroaromatic five-membered ring to bridge two substituted phenyl moieties. However, unlike PTC124, **5** does not form an MAI through reaction with ATP. In fact ATP is not bound to FLuc in the presence of **5**, presumably due to protrusion of the isopropyl alcohol of **5** into space normally occupied by the terminal phosphoryl groups of ATP. Furthermore, the deep pocket present within FLuc, which is not fully occupied by either luciferin or PTC124, is exploited by **5** and evident by the extension of the second isopropyl alcohol on the opposite end of **5** reaching into this deep pocket (Figure 6). These findings illustrate the chemical diversity capable of interacting with this pocket and help to further explain the frequent occurrence of small molecule modulators of FLuc identified in chemical-screening libraries.

In future uses of NPE libraries, we are exploring incorporation of a titration-based screening paradigm across common assay platforms, e.g., in biochemical target-based screens across gene families (Veith et al., 2009) or in cell-based assays using the same detection output (Yuan et al., 2009). Such data would be augmented when properly designed assay panels are configured that differentiate between NPEs bearing a technically based inhibition pattern versus NPEs that are genuinely active on a biologically relevant mechanism (e.g., contain orthogonal assay pairs) (Inglese et al., 2007). The combination of qHTS with panels containing both parallel and orthogonally designed assays should facilitate the identification of NPs selective for the target or cellular pathway being explored from NPE libraries, in the same way this strategy is used for synthetic chemical libraries (Johnson et al., 2009; Xia et al., 2009).

We view this study as a work in progress aimed at defining an improved process for exploring the vast potential of NPs held within complex mixtures. Focusing here on the use of microbial-derived NPs prefractionated to remove the majority of HTS-interfering components, we have employed the pharmacological-resolving power of qHTS to reveal apparent IC_{50} values from these mixtures. By using a pattern of high-quality CRCs (curve class 1a), we demonstrated that a reproducible activity could be targeted from among many "active" NPEs and reduced to a candidate NPE for follow-up dereplication. Incorporating the wealth of metadata associated with NPEs can further enhance the CRC information. Metadata information includes strain, growth conditions, broth or cellular fraction, and solvent extraction method, which can all be used to guide the choice of fractions for follow-up. For this purpose we developed a browser to help visualize and track the metadata information

(see Experimental Procedures for full description). In this study we were able to identify a series of aspulvinones that selectively inhibited the *Photinus pyralis* FLuc, showing that the widespread modulation of FLuc activity observed in synthetic chemical libraries (Auld et al., 2008b) extends to NPEs as well. By applying the strategy we have outlined here, we are now in a position to improve the efficiency of NPE screening in drug discovery applications across a wide range of human and animal disease targets.

SIGNIFICANCE

The natural world remains a source of great chemical diversity producing compounds demonstrated to have tremendous medicinal value. However, their use in discovery efforts has been decreasing because HTS approaches that may be sufficient for testing of pure synthetic compounds remain suboptimal for complex mixtures such as natural product extracts (NPEs). For example typical extracts may harbor optically active pigments with relatively low concentrations of bioactive substances. This interference can prevent effective testing of crude NPEs at high concentrations in sensitive fluorescent or luminescent HTS-based assays. Therefore, both the preparation of the NPE and enhancements to the screening paradigm are needed. Increasing efficiency for assessing the biological activity of secondary metabolites derived from plants, and macro- and microorganisms will likely reenergize their use in lead discovery efforts. Here, a library of prefractionated NPEs leads to rapid identification of active NP molecules. Quantitative HTS (qHTS) enabled effective investigation of the extracts because the technique integrates testing of a concentration series that can accommodate relatively high apparent micromolar concentrations for the detection of low-abundance compounds. NPEs containing relevant bioactive molecules were revealed by sigmoidal CRCs and readily discriminated from inactive samples. Inclusion of cross-validation assays for a specific pathway or target, or a common assay platform for testing multiple cell lines or targets, improved identification of target-directed or target-selective NPEs, respectively. Given the effort required to process active fractions derived from NPEs, the general approach described here should facilitate the discovery of NPs employing ongoing advances in assay development and functional genomics.

EXPERIMENTAL PROCEDURES

Preparation of NPE Libraries and Control Plates

Isolated strains from Costa Rican marine sediments were cultured (100 ml) in two different media (see below). After cell growth, broth was separated by centrifugation and agitated by shaking overnight with Amberlite XAD-16, which was further extracted with CH_3OH, acetone, and EtOAc sequentially. The NPEs were transferred to the NIH Chemical Genomics Center (NCGC) on dry ice in 384-well plates containing 60 μl of a 15 mg/ml solution in DMSO. The NCGC reformatted the extracts in the HTS compound management core using the qHTS dilution paradigm (Yasgar et al., 2008) resulting in an inter-plate or "through-plate" titration series in 1536-well format in DMSO (Figure S1B). Briefly, fifty 384-well NPE library plates were titrated using a 1:5 dilution factor, to generate a seven-point titration series. The resulting three hundred fifty 384-well plates were compressed to ninety-one 1536-well plates for screening, with the first 4 columns of each plate reserved for assay-specific

controls. Unique identifiers were auto-generated by registering the sample IDs and strain origins from an accompanying data file into ActivityBase (ID Business Solutions Ltd., Guildford, UK). ActivityBase was also used to track the sample locations in the bar-coded 384-well plates.

Controls were added from columns 1–4 of a separate 1536-well compound plate. Depending on the assay, titrations, maximum/minimum and/or neutral controls are used, for example: columns 1–2, 16-point titrations in duplicate of test compounds starting at 20 mM in DMSO; column 3, neutral control (DMSO); and column 4, control inhibitor (20 mM resveratrol).

qHTS and Follow-up Data Analysis

The NPE 1536-well titration archive was tested against assays of the MLPCN using an automated qHTS process described previously (Inglese et al., 2006; Michael et al., 2008) and described further in the Supplemental Experimental Procedures.

Curve Classification Analysis

The curve classification used is the same as the one described elsewhere (Inglese et al., 2006). Briefly, CRCs are categorized into four classes. Class 1 contains complete CRC having both upper and lower asymptotes and r^2 values >0.9. Class 2 contains incomplete CRCs lacking the high-concentration asymptote and shows r^2 values >0.9. Being supported by a single concentration having activity, class 3 curves are considered low confidence. For class 3 the minimal acceptable activity is set at 3 SD of the mean activity calculated as described above. Curves are classified as negative or positive, depending on whether they exhibit a signal decrease (apparent inhibition) or increase (apparent activation). Finally, class 4 contains compounds that do not show any activity that define a CRC and are, therefore, classified as inactive. Active compounds were identified as a range of curve classes from 1 through 3 to select for compounds showing signal decreases.

Luciferase Assays

Vibrio fischeri luciferase (VLuc) was purchased from Sigma-Aldrich (catalog #L8507), which is a partially purified preparation of VLuc that contains the necessary NADH/NADPH-dependent FMN reductases. Luciferase from *Luciola mingrelica* (LmLuc) was purchased from Sigma-Aldrich (catalog #L4899). Purified wild-type luciferase from *Photinus pyralis* (FLuc) was obtained from Sigma-Aldrich (catalog #L9506), and purified Ultra-Glo luciferase was obtained from Promega (Auld et al., 2009b). *Renilla reniformis* luciferase (RLuc) was purchased from Nanolight.

The 1536-well RLuc and FLuc assays were performed as previously described (Auld et al., 2008b, 2009a) using either 5μM coelenterazine or 10 μM D-luciferin and ATP, respectively. The assay for LmLuc used the same protocol as FLuc with a final concentration of 5 nM LmLuc enzyme. The assay for Ultra-Glo also used 10 μM D-luciferin and ATP and was performed as described (Auld et al., 2009b). The assay for the FMN-dependent luciferase VLuc followed the procedure described in Lavi et al. (1981) but used a miniaturized assay volume of 4 μl in 1536-well plates. For the assay, 2 μl of substrate buffer (0.1 M sodium phosphate [pH 7.0], 0.005% decanal, 0.1% BSA, 0.1 mM NADH, and 2 μM FMN) was dispensed into Kalypsys white medium binding 1536-well plates. Compounds were then added using a Kalypsys pin tool. The assay was started by adding enzyme buffer (0.1 M sodium phosphate [pH 7.0], 0.2 μM VLuc), and the luminescent signal was read immediately on a PerkinElmer ViewLux (180 s exposure, 6× binning).

Fungal Isolation, Identification, and Cultivation

The fungus *Aspergillus* sp. (strain 05545) was isolated from a marine sponge collected in 2005 in La Cruz, Costa Rica, by J. Cortez (authorization accession permit R-CM-08-2006-OT for samples donated by CIMAR to INBio, collection permit 106-2005-SINAC). The isolated fungus was preserved with 20% glycerol at −80°C. It was cultured in ISP2 media (10 g of malt extract, 4 g of yeast extract, 4 g of dextrose, and 30 g of NaCl/l of distilled water) at 28°C on a rotary shaker at 200 rpm in five replicates of 2.5 l Fernbach flasks, each containing 1 l of culture media.

Extraction and Isolation

After 8 days of culture, *Aspergillus* sp. (strain 05545) fungus cells were harvested by centrifugation at 3000 × g, sonicated, and extracted with MeOH.

The culture broth was extracted by adding 20 g/l Amberlite XAD-16. After shaking overnight, the resin was collected and washed with 1 l of DI water before it was sequentially extracted with methanol, acetone, and ethyl acetate. The resulting extracts were filtered and concentrated to obtain 1.82, 0.87, and 0.26 g of crude extract, respectively. The MeOH extract was subjected to successive chromatography procedures. First, a medium-pressure reversed-phase LOBAR B (Ø = 25 × 310 mm) LiChroprep column was used, eluted with MeOH-H$_2$O (7:3) to yield three active fractions: b, c, and d. Fractions b (539 mg), c (510 mg), and d (364 mg) were further subjected to HPLC purification on a XBridge Prep C18 column (Ø = 10 × 250 mm) with CH$_3$CN-H$_2$O gradient. The subfractions were further purified on the same column using phase MeOH-H$_2$O gradient as the mobile phase to give: aspulvinone E (**1**, 3.2 mg); aspulvinone F (**2**, 40 mg); aspulvinone H (**3**, 6 mg); aspulvinone I-CR (**4**, 13 mg); aspulvinone J-CR (**5**, 4.2 mg); aspulvinone K-CR (**6**, 7.4 mg); aspulvinone L-CR (**7**, 1.8 mg); aspulvinone M-CR (**8**, 2 mg); aspulvinone N-CR (**9**, 5 mg); butyrolactone I (**10**, 1.6 mg); butyrolactone III (**11**, 6.6 mg); and benzofuran (**12**, 1.8 mg).

General Experimental Procedures for NP Structure Elucidation
Optical rotations were measured on an AUTOPOL III Polarimeter. IR spectra were recorded with a PerkinElmer BX FT-IR infrared spectrometer using NaCl plates. Mass spectra were carried out with a Micromass AutoSpec Ultima Magnetica mass spectrometer. ^{1}H, ^{13}C, and 2D NMR spectra were recorded in CD$_3$OD on a Varian INOVA 600 MHz NMR spectrometer at 600 MHz for ^{1}H and 150 MHz for ^{13}C, using TMS as an internal standard. Medium-pressure chromatography was performed using prepacked columns, including LOBAR GRÖBE B (Ø 25 × 310 mm) LiChroprep RP-18 from MERCK. HPLC separations were performed on a Beckman Coulter system (Fullerton, CA) equipped with a diode-array detector, using a XBridge Prep C18 column (Ø = 10 × 250 mm). TLC was performed using TLC silica gel 60 F254 from EMD, and plates were visualized by spraying with PMA and heating. Specific characterization and spectral data for Aspulvinone F (**2**), Aspulvinone I-CR (**4**), Aspulvinone J-CR (**5**), Aspulvinone K-CR (**6**), Aspulvinone L-CR (**7**), Aspulvinone M-CR (**8**), and Aspulvinone N-CR (**9**) are provided in Supplemental Experimental Procedures.

Crystallographic Data of Aspulvinone F-CR (2)
Yellow, C$_{132}$H$_{156}$Na$_4$O$_{36}$, monoclinic, space group $P2_1$, a = 21.470(6) Å, b = 10.861(3) Å, c = 27.520(7) Å, β = 93.705(4)°, V = 6404(3) Å^3, Z = 2, crystal size 0.32 × 0.28 × 0.08 mm^3. The intensities of the reflections were collected by means of a Bruker APEX II CCD diffractometer (Mo$_{K\alpha}$ radiation, λ = 0.71073 Å), and equipped with an Oxford Cryosystems nitrogen flow apparatus. The collection method involved 0.5° scans in ω at 26° in 2θ. Data integration down to 0.82 Å resolution was carried out using a Bruker SAINT V7.46 A diffractometer (Madison, WI) with reflection spot size optimization. Absorption corrections were made with the Bruker program TWINABS (Madison, WI). The structure was solved by the direct methods procedure and refined by least-squares methods again F^2 using SHELXS-97 and SHELXL-97 (Sheldrick, 2008). Nonhydrogen atoms were refined anisotropically, and hydrogen atoms were allowed to ride on the respective atoms. The Ortep plots were produced with SHELXL-97 program, and the other drawings were produced with Accelrys DS Visualizer 2.0 (San Diego, CA).

Cocrystallization and Data Collection for FLuc-Aspulvinone J-CR
Luciferase from *Photinus pyralis* was purchased from Sigma-Aldrich (catalog #L9506, lot #017K74201), and concentrated to 10.2 mg/ml in 200 mM (NH$_4$)$_2$SO$_4$, 1 mM EDTA, 1 mM DTT, 10% glycerol, 25% ethylene glycol, and 25 mM Tris [pH 7.8] as previously described (Conti et al., 1996). Apo crystals were obtained at 4°C in CombiClover, Jr. (Emerald BioSystems) sitting drop plates using equal volumes of protein and crystallization solution (25% (v/v), PEG 400, 20% (v/v) PEG 3350, 0.1 M MgCl$_2$, 0.1 M Tris [pH 8.5], Precipitat Synergy #41, Emerald BioSystems) equilibrated against 100 μl of the latter. Apo crystals were soaked for 2.5 hr in the presence of 10 mM NCGC183923 (Aspulvinone J-CR (**5**)) and 10 mM NCGC183923 (Aspulvinone J-CR (**5**))/2.5 mM ATP dissolved in crystallization solution. Diffraction data were collected at 100 K at the Advanced Photon Source (APS) IMCA-CAT beamline 17-ID using a Dectris Pilatus 6 M pixel array detector.

Structure Solution and Refinement
Diffraction data were integrated and scaled with XDS (Kabsch, 1988) and Scala (Evans, 2006), respectively. The protein-only coordinates from a previously determined luciferase structure (using PDB: 3IES) were used for initial refinement against the processed diffraction data. Refinement and model building were carried out with PHENIX (Adams et al., 2010) and Coot (Emsley and Cowtan, 2004), respectively. Disordered side-chain residues were truncated to the point to which electron density could be observed. Structure validation was conducted with MolProbity (Lovell et al., 2003), and figures were prepared with CCP4mg (Potterton et al., 2004). Following initial refinement, prominent electron density (Fo-Fc) consistent with NCGC183923 was observed in the active site for the inhibitor and inhibitor/ATP-soaked crystals. However, no electron density consistent with ATP was observed for the latter sample. Final structure refinement was conducted using the diffraction data collected for the NCGC183923/ATP-soaked crystal because it diffracted to the highest resolution. Crystallographic data are provided in Table S2.

NPE Informatics Browser
Our current primary screening data visualization platform is a two-stage solution implemented in LabVIEW (Austin, TX): a parser that collates the qHTS data by microbial strain variant, and a browser that displays the collated data as a global overview of assays tested against the NPE collection (see Supplemental Experimental Procedures).

ACCESSION NUMBERS

Coordinates and structure factors of the 1.7 Å resolution structure of a firefly luciferase-aspulvinone J-CR (**5**) inhibitor complex are available at PDB ID code 3RIX.

SUPPLEMENTAL INFORMATION

Supplemental Information includes Supplemental Experimental Procedures, four tables, and thirty-two figures and can be found with this article online at doi:10.1016/j.chembiol.2011.08.011.

REFERENCES

Adams, P.D., Afonine, P.V., Bunkóczi, G., Chen, V.B., Davis, I.W., Echols, N., Headd, J.J., Hung, L.W., Kapral, G.J., Grosse-Kunstleve, R.W., et al. (2010). PHENIX: a comprehensive Python-based system for macromolecular structure solution. Acta Crystallogr. D Biol. Crystallogr. 66, 213–221.

Auld, D.S., Thorne, N., Nguyen, D.T., and Inglese, J. (2008a). A specific mechanism for nonspecific activation in reporter-gene assays. ACS Chem. Biol. 3, 463–470.

Auld, D.S., Southall, N.T., Jadhav, A., Johnson, R.L., Diller, D.J., Simeonov, A., Austin, C.P., and Inglese, J. (2008b). Characterization of chemical libraries for luciferase inhibitory activity. J. Med. Chem. 51, 2372–2386.

Auld, D.S., Thorne, N., Maguire, W.F., and Inglese, J. (2009a). Mechanism of PTC124 activity in cell-based luciferase assays of nonsense codon suppression. Proc. Natl. Acad. Sci. USA 106, 3585–3590.

Auld, D.S., Zhang, Y.Q., Southall, N.T., Rai, G., Landsman, M., MacLure, J., Langevin, D., Thomas, C.J., Austin, C.P., and Inglese, J. (2009b). A basis for reduced chemical library inhibition of firefly luciferase obtained from directed evolution. J. Med. Chem. 52, 1450–1458.

Auld, D.S., Lovell, S., Thorne, N., Lea, W.A., Maloney, D.J., Shen, M., Rai, G., Battaile, K.P., Thomas, C.J., Simeonov, A., et al. (2010). Molecular basis for the high-affinity binding and stabilization of firefly luciferase by PTC124. Proc. Natl. Acad. Sci. USA 107, 4878–4883.

Baell, J.B., and Holloway, G.A. (2010). New substructure filters for removal of pan assay interference compounds (PAINS) from screening libraries and for their exclusion in bioassays. J. Med. Chem. 53, 2719–2740.

Begley, M.J., Gedge, D.R., Knight, D.W., and Pattenden, G. (1979). Aspulvinones, a new class of natural products from *Aspergillus terreus*. Re-investigation of structures by X-ray crystallographic and spectroscopic analysis. J. Chem. Soc. Perkin Trans. I, 77–83.

Burley, S.K., and Petsko, G.A. (1985). Aromatic-aromatic interaction: a mechanism of protein structure stabilization. Science 229, 23–28.

Burley, S.K., and Petsko, G.A. (1988). Weakly polar interactions in proteins. Adv. Protein Chem. 39, 125–189.

Butler, M.S. (2008). Natural products to drugs: natural product-derived compounds in clinical trials. Nat. Prod. Rep. 25, 475–516.

Carlson, E.E. (2010). Natural products as chemical probes. ACS Chem. Biol. 5, 639–653.

Conti, E., Lloyd, L.F., Akins, J., Franks, N.P., and Brick, P. (1996). Crystallization and preliminary diffraction studies of firefly luciferase from *Photinus pyralis*. Acta Crystallogr. D Biol. Crystallogr. 52, 876–878.

Ding, Y., de Wet, J.R., Cavalcoli, J., Li, S., Greshock, T.J., Miller, K.A., Finefield, J.M., Sunderhaus, J.D., McAfoos, T.J., Tsukamoto, S., et al. (2010). Genome-based characterization of two prenylation steps in the assembly of the stephacidin and notoamide anticancer agents in a marine-derived *Aspergillus* sp. J. Am. Chem. Soc. 132, 12733–12740.

Donnelly, D.M.X., Fukuda, N., Kouno, I., Martin, M., and O'Reilly, J. (1988). Dihydrobenzofurans from *Heterobasidion annosum*. Phytochemistry 27, 2709–2713.

Emsley, P.K.C., and Cowtan, K. (2004). Coot: model-building tools for molecular graphics. Acta Crystallogr. D Biol. Crystallogr. 60, 2126–2132.

Evans, P. (2006). Scaling and assessment of data quality. Acta Crystallogr. D Biol. Crystallogr. 62, 72–82.

Harvey, A.L. (2007). Natural products as a screening resource. Curr. Opin. Chem. Biol. 11, 480–484.

Huang, H.Y., Ishikawa, T., Peng, C.F., Tsai, I.L., and Chen, I.S. (2008). Constituents of the root wood of *Zanthoxylum wutaiense* with antitubercular activity. J. Nat. Prod. 71, 1146–1151.

Inglese, J., Auld, D.S., Jadhav, A., Johnson, R.L., Simeonov, A., Yasgar, A., Zheng, W., and Austin, C.P. (2006). Quantitative high-throughput screening: a titration-based approach that efficiently identifies biological activities in large chemical libraries. Proc. Natl. Acad. Sci. USA 103, 11473–11478.

Inglese, J., Johnson, R.L., Simeonov, A., Xia, M., Zheng, W., Austin, C.P., and Auld, D.S. (2007). High-throughput screening assays for the identification of chemical probes. Nat. Chem. Biol. 3, 466–479.

Johnson, R.L., Huang, R., Jadhav, A., Southall, N., Wichterman, J., MacArthur, R., Xia, M., Bi, K., Printen, J., Austin, C.P., and Inglese, J. (2009). A quantitative high-throughput screen for modulators of IL-6 signaling: a model for interrogating biological networks using chemical libraries. Mol. Biosyst. 5, 1039–1050.

Kabsch, W. (1988). Automatic indexing of rotation diffraction patterns. J. Appl. Crystallogr. 21, 67–72.

Koehn, F.E., and Carter, G.T. (2005). Rediscovering natural products as a source of new drugs. Discov. Med. 5, 159–164.

Lam, K.S. (2007). New aspects of natural products in drug discovery. Trends Microbiol. 15, 279–289.

Lavi, J.T., Lövgren, T.N.-E., and Raunio, R.P. (1981). Comparison of luminous bacteria and their bioluminescence-linked enzyme activities. FEMS Microbiol. Lett. 11, 197–199.

Li, J.W., and Vederas, J.C. (2009). Drug discovery and natural products: end of an era or an endless frontier? Science 325, 161–165.

Lovell, S.C., Davis, I.W., Arendall, W.B., 3rd, de Bakker, P.I., Word, J.M., Prisant, M.G., Richardson, J.S., and Richardson, D.C. (2003). Structure validation by Calpha geometry: phi,psi and Cbeta deviation. Proteins 50, 437–450.

Michael, S., Auld, D., Klumpp, C., Jadhav, A., Zheng, W., Thorne, N., Austin, C.P., Inglese, J., and Simeonov, A. (2008). A robotic platform for quantitative high-throughput screening. Assay Drug Dev. Technol. 6, 637–657.

Newman, D.J. (2008). Natural products as leads to potential drugs: an old process or the new hope for drug discovery? J. Med. Chem. 51, 2589–2599.

Newman, D.J., and Cragg, G.M. (2009). Natural product scaffolds as leads to drugs. Future Med. Chem. 1, 1415–1427.

Niu, X., Dahse, H.M., Menzel, K.D., Lozach, O., Walther, G., Meijer, L., Grabley, S., and Sattler, I. (2008). Butyrolactone I derivatives from *Aspergillus terreus* carrying an unusual sulfate moiety. J. Nat. Prod. 71, 689–692.

Ojima, N., Takenaka, S., and Seto, S. (1975). Structures of pulvinone derivatives from *Aspergillus terreus*. Phytochemistry 14, 573–576.

Parvatkar, R.R., D'Souza, C., Tripathi, A., and Naik, C.G. (2009). Aspernolides A and B, butenolides from a marine-derived fungus *Aspergillus terreus*. Phytochemistry 70, 128–132.

Potterton, L., McNicholas, S., Krissinel, E., Gruber, J., Cowtan, K., Emsley, P., Murshudov, G.N., Cohen, S., Perrakis, A., and Noble, M. (2004). Developments in the CCP4 molecular-graphics project. Acta Crystallogr. D Biol. Crystallogr. 60, 2288–2294.

Rao, K.V., Sadhukhan, A.K., Veerender, M., Ravikumar, V., Mohan, E.V., Dhanvantri, S.D., Sitaramkumar, M., Babu, J.M., Vyas, K., and Reddy, G.O. (2000). Butyrolactones from *Aspergillus terreus*. Chem. Pharm. Bull. 48, 559–562.

Sheldrick, G.M. (2008). A short history of SHELX. Acta Crystallogr. A 64, 112–122.

Shukla, S.J., Nguyen, D.T., Macarthur, R., Simeonov, A., Frazee, W.J., Hallis, T.M., Marks, B.D., Singh, U., Eliason, H.C., Printen, J., et al. (2009). Identification of pregnane X receptor ligands using time-resolved fluorescence resonance energy transfer and quantitative high-throughput screening. Assay Drug Dev. Technol. 7, 143–169.

Sugiyama, H., Ojima, N., Kobayashi, M., Senda, Y., Ishiyama, J., and Seto, S. (1979). C-13 NMR spectra of Aspulvinones. Agric. Biol. Chem. 43, 403–404.

Thorne, N., Auld, D.S., and Inglese, J. (2010a). Apparent activity in high-throughput screening: origins of compound-dependent assay interference. Curr. Opin. Chem. Biol. 14, 315–324.

Thorne, N., Inglese, J., and Auld, D.S. (2010b). Illuminating insights into firefly luciferase and other bioluminescent reporters used in chemical biology. Chem. Biol. 17, 646–657.

Veith, H., Southall, N., Huang, R., James, T., Fayne, D., Artemenko, N., Shen, M., Inglese, J., Austin, C.P., Lloyd, D.G., and Auld, D.S. (2009). Comprehensive characterization of cytochrome P450 isozyme selectivity across chemical libraries. Nat. Biotechnol. 27, 1050–1055.

Xia, M., Huang, R., Guo, V., Southall, N., Cho, M.H., Inglese, J., Austin, C.P., and Nirenberg, M. (2009). Identification of compounds that potentiate CREB signaling as possible enhancers of long-term memory. Proc. Natl. Acad. Sci. USA *106*, 2412–2417.

Yasgar, A., Shinn, P., Jadhav, A., Auld, D., Michael, S., Zheng, W., Austin, C.P., Inglese, J., and Simeonov, A. (2008). Compound management for quantitative high-throughput screening. JALA Charlottesv. Va. *13*, 79–89.

Ye, L., Buck, L.M., Schaeffer, H.J., and Leach, F.R. (1997). Cloning and sequencing of a cDNA for firefly luciferase from *Photuris pennsylvanica*. Biochim. Biophys. Acta *1339*, 39–52.

Yuan, J., Johnson, R.L., Huang, R., Wichterman, J., Jiang, H., Hayton, K., Fidock, D.A., Wellems, T.E., Inglese, J., Austin, C.P., and Su, X.Z. (2009). Genetic mapping of targets mediating differential chemical phenotypes in *Plasmodium falciparum*. Nat. Chem. Biol. *5*, 765–771.